ORIGINAL ARTICLE

Identifying the lead angle limit to achieve required surface roughness in ball-end milling

Matej Pesice[1] · **Petr Vavruska**[1] · **Jiri Falta**[2] · **Pavel Zeman**[2] · **Jan Maly**[2]

Abstract

When milling generally shaped surfaces with a ball-end milling tool, machined surface roughness and accuracy as well as machining productivity are often monitored. Improving one of these parameters often causes a decrease in the other monitored parameters. Therefore, knowing possible ways of influencing these parameters is important for achieving the optimum result, if possible, in all requirements. A deep understanding of how some technological parameters influence finished surface roughness is still lacking, as well as detailed knowledge of the relationships among some roughness parameters. In response, an experiment entailing machining of planar samples at different orientation angles was carried out to identify the influence of the studied parameters on the transverse roughness of the final surface. A finding was made that the resulting surface roughness is dependent on the cutting edge geometry of the particular ball-end milling tools used, and the achieving of the required surface roughness can be guaranteed by setting the specific lead angles. Furthermore, it was verified that a minimum lead angle limit can be found based on the geometric properties of the specific milling tool, and the relationship between the evaluated roughness parameters Ra and Rz was found as well.

Keywords Milling · Surface roughness · Ball-end-milling tool · Scallop · Real cutting diameter · Lead angle

1 Introduction

When milling generally shaped surfaces, the machined surface quality, shape and dimensional accuracy of the final surface and machining productivity are very important aspects of finishing machining. Roughness, which plays the largest role in evaluation of machined surface quality, is a directly measured parameter that must be achieved when machining a part. Tools with a circular cutting edge, known as ball-end mills, are used to finish shaped surfaces. When a surface is point milled using this type of tool, the main geometric parameters that determine the resulting surface

roughness are the tool diameter and the spacing between the single passes of the toolpath (step-over). These parameters determine the height of the remaining material on the machined surface, known as the scallop [1]. The structure of the final surface is also influenced by factors such as the choice of cutting speed and feed rate. The surface roughness can be evaluated in the direction of tool movement (along the tool path—longitudinal roughness) or perpendicular to the direction of tool movement (across the toolpath—transverse roughness). Based on the nature of the shape of the remaining material, the scallop parameter can be compared to the resulting roughness Rz (roughness depth parameter, defined by ISO 4287), evaluated perpendicular to the direction of tool movement. The surface roughness in the direction of tool movement is mainly determined by the tool rotation and feed per tooth. If the cutting conditions are set optimally, the roughness perpendicular to the direction of tool movement has a predominant influence on the resulting surface. Thus, the scallop is a parameter that can be selected during machining operation setup in the CAM system and used to determine the expected machined surface roughness. However, there is no direct information about the relationship between the scallop parameter and the resulting

✉ Matej Pesice
M.Pesice@rcmt.cvut.cz

[1] Department of Production Machines and Equipment (RCMT), Faculty of Mechanical Engineering, Czech Technical University in Prague, Technicka Street 4, 16607 Prague 6, Prague, Czech Republic

[2] Department of Production Machines and Equipment, Faculty of Mechanical Engineering, Centre of Advanced Aerospace Technology, Czech Technical University in Prague, Technicka Street 4, 16607 Prague 6, Prague, Czech Republic

Ra value (the average arithmetic roughness according to ISO 4287), which is often the only defined parameter to be achieved after surface machining. The relationship between the parameters *Rz* and *Ra* is addressed in DIN 4763, which provides only a relatively wide range of values (not very detailed) and several papers can be found describing experiments with data measurements monitoring a narrow range of conditions [2–5]. Other parameters that are not included in the scallop calculation also need to be taken into account and examined through experiments. The experiments mentioned below demonstrate that changing some technological parameters results in a different surface quality (parameter *Ra*) for the same scallop value. These parameters include, for example, cutting speed, tool orientation angle, tool diameter, the choice of material to be machined and the relationship to tool wear.

Other parameters that are used when setting the toolpath for machining shaped surfaces are the lead angle and the tilt angle of the tool axis. The lead and tilt angles directly affect the cutting speed achieved with a specific spindle speed at the point of contact with the material. The smaller the tool lead angle, the less material is machined at the effective tool diameter, and therefore the lower the cutting speed. If machining is carried out with a zero tool axis orientation angle, the material is removed by the tool area close to the tool centre where the effective diameter is very small; and therefore, the cutting speed decreases rapidly. A low cutting speed and low effective diameter have a negative impact on the resulting transverse roughness [6, 7]. This is one of the reasons why a lead angle or tool tilting is used in milling. However, some specific machining cases do not allow for significant lead and tilting angles and only angles in the order of units of degrees are possible (e.g. milling of narrow inter-blade spaces). In three-axis milling of a shaped area, where the tool orientation is constant (perpendicular to the plane of the machine tool table), the angle of orientation of the tool from the workpiece surface is determined by the particular shape of the workpiece (its curvature and orientation at a given point). Thus, at certain toolpath points, the near centre of the tool is used during machining. Batista et al. [6] experimentally verified the surface finish when machining WNr 1.2367/X38CrMoV5-3 steel with a zero-tilt angle cutter. Cycloid-shaped traces are visible on the workpiece surface which correspond to the ploughing of the material. These cycloids have a constant pitch, which is determined by the feed rate. A similar finding was made by Mali [8], who investigated the effect of changing the direction of the point milling toolpath and cutting conditions during three-axis milling of a shaped workpiece of Duralloy EN AW 7075. Mikó and Zentay [9] presented a geometric approach to predict the contact point and working values resulting from it when performing a 3-axis ball-end milling of the freeform surface. The author touches the topics such as working

diameter, low cutting speed and the geometrical point of view in general. An optimization approach is proposed to preserve the optimal cutting diameter by changing the toolpath strategy for this basic milling case.

de Souza [10] investigated force loads when machining an AISI P20 steel-shaped workpiece using a ball-end mill. The experiment showed that the highest force load occurs in the tool centre where the material is formed rather than machined. By increasing the cutting speed, the area of this significant increase in cutting forces near the tool centre can be narrowed and the force load at all locations of the shaped workpiece can also be reduced. The effective milling diameters are also monitored as a function of the machining direction at a particular location. A similar experiment was also carried out by Scandiffio [11] when milling AISI D6 tool steel. He discussed the relationship of the effective cutting diameter to different milling directions, force loads and the resulting surface roughness. For three tilting angles, pulling the tool resulted in lower roughness and lower cutting forces than when it was pushed. Beno obtained similar findings when machining a generally shaped surface [12], observing the resultant quality when the rows were machined in different directions with respect to the workpiece shape. Aspinwall et al. [13] demonstrated the effect of cutter orientation on the machinability of Inconel 718 through experiments. The orientation of the tool axis relative to the machined surface was defined by a fixed angle of 45°. The effect of different surface rows (pulling, pushing) was investigated and for comparison the surface was machined at a 0° tool orientation (three-axis milling). The experiment showed that the toolpath direction and tool axis orientation have a clear effect on tool life, cutting forces and the resulting surface roughness. Wojciechowski et al. drew similar conclusions [14, 15]. Vavruska et al. [16] proposed an algorithm for calculating the cutting speed and feed rate depending on the current effective diameter at a specific location on the workpiece, which leads to achievement of selected cutting conditions. Käsemodel et al. [17] subsequently carried out a machining experiment using a new computational algorithm based on previous findings. Erdim et al. [18] optimised the feed on the shape path by calculating the material removal at a specific location according to the contact point in order to increase productivity (reduction of machining time). Rybicki [19] not only adopted a similar approach but also varied spindle speed in addition to feed rate and achieved a lower tool load and constant roughness of the machined surface alongside a reduction of machining time.

Matras and Zebala [20] addressed machining of hardened steel with a CBN ball mill. He proposed a cutting force prediction algorithm that takes into account the tool contact point at a specific location of the shaped workpiece during three-axis milling. He optimised cutting conditions, supported by an experiment verifying cutting condition settings

(especially feed rate) and the effect of this change on cutting force magnitude. Lazoglu et al. [21] optimised the machining path to achieve the lowest possible force load. The proposed force optimisation is more suitable for semi-finishing operations since toolpath modification affects the resulting surface texture. Costes and Moreau [22] predicted surface roughness based on changes in the position on the shaping toolpath. The author predicted tool vibration locations and experimentally verified the calculations using laser sensors. The roughness measurements correspond to the calculations. No et al. [23] focused on a reverse engineering simulation of cutting forces and tool orientation for selected cutting conditions. Data from a 3D scan of the tool (cylindrical cutter) were used for the prediction, for which the scanned points around the cutting edge are essential. Tunc [24] proposed a novel approach for automatic modification of the 5-axis milling toolpaths. The simulation process evaluates the limit factor from different sources (cutting forces, stability, scallop height calculation) and changes the toolpath for improving the result and also for reducing the machining time. The approach benefits from the new process simulation tools.

There are also various analytical (mathematical prediction) studies that aim to predict the resulting surface roughness. Mikó et al. [25] defined the mathematical relationships for predicting scallop height depending on input parameters such as toolpath density or lead angle. It is a prediction model of the scallop that emerges during changes to the toolpath spacing (also called step-over). Chen et al. [1] modelled the longitudinal and transversal surface roughness with respect to changes of the feed per tooth. While the cutter diameter changed, the step-over was kept constant and the feed per tooth was increased. Thus, there is a decrease in Rz in the transverse direction (scallop parameter in the design) but an increase in longitudinal roughness (an effect of increasing the feed rate). In his study, Shchurov and Al-Taie [26] alluded to the problem of projecting the toolpath onto a curved surface (specifically a spherical canopy). He proposed a mathematical model that ensures uniform distribution of the toolpath passes on the workpiece shape in order to achieve constant spacing and therefore constant roughness over the entire curved surface. In summary, he concluded that given the vastness of the problem, the development of a mathematical algorithm capturing all cases of curvature change (convex–concave transitions, etc.) requires further work. Similarly, Liu [27] improved his previous mathematical algorithm [28] which aims to adjust the CL data to obtain the best possible scalloped shape surface in terms of the scallop parameter. Yang et al. [29] used the NURBS method to simulate the residual surface after sphere milling. He observed the effect of the machined surface curvature on the resulting roughness and discussed the relationship between tool compliancy and tool vibration at larger tilt angles. Quinsat et al. [30] proposed a simulation model

of the 3D topography for three-axis machining of the free-form surface when using a ball-end mill. The model considers actual curvature of the surface in specific point and its relation with the tool axis direction. The resulting surface quality is also put into context with the cutting conditions and tool parameters (such as tool diameter, feed rate), but it considers just ideal tool geometry. Sekine [31] focused on the calculation of the scallop height when milling with ball-end and toroidal tools. The tool diameters were taken into account, and also cutting speed was put into context with the material removal thanks to geometrical consideration. In another study, this author [32] observed toroidal mill inclination angle influence on the geometrical consequence of the chip removal. The study proposes optimal inclination angle for best results considering material removal for observed cutting conditions. Lofti et al. [33] proposed an approach to model the chip thickness in multi-axis ball-end milling. The model includes the rotation of the cutting edge considering inclination angle in various directions for given feed rate setting. The aim was to model the cutting forces based on the material removal knowledge, and the experimental results showed good agreement with the model assumptions. Zhang et al. [34] come with the new approach to optimise the tool orientation during 5-axis ball-end milling of the plane, cylindrical and spherical surfaces. The optimization considers cutter runout, two-workpiece cutting direction relation and proposes also force prediction algorithm. The model aims to improve machining accuracy and efficiency by controlling the inclination angle setting. Similar approach and intent are present in the study of Jang et al. [35]. The authors used quadratic equations for optimization of the inclination angles when point milling with a flat-end cutter.

Changing the tool orientation angle as well as the milling direction plays an important role when machining difficult-to-cut materials. Matras [36] investigated the dependence of the resulting surface roughness on the selected angle of pulling/pushing when machining 16MnCr5 steel. The angle is varied in 10° increments from −90° to 90° (0°—machining through the centre of the tool). The results showed that the worst roughness occurred near 0°. However, the step of changing the tool tilt angle is quite coarse for a detailed analysis of the behaviour of the resulting surface roughness. Stejskal et al. [37] conducted an experiment machining Duralloy EN AW 7075 and duplex steel DIN 1.4462 and focused on the relationship between the contact point parameter of the ball-end mill and the actual cutting speed. From the surface roughness measurements of the planar specimens, they found an approximate limiting lead angle value from which the resulting surface finish remains unchanged as the lead angle increases. Here, the lead angle was varied near the tool centre in small increments (1°) but the quality was assessed from a visual perspective rather than by comparison with the theoretical scallop value from the CAM system. The findings led to the

development of an optimization algorithm that adjusts the tool orientation vector on the machining toolpath of the general shape surface. Sadilek and Cep [38] observed the effect of the tool inclination angle in four directions (i.e. also conventional and climb cut) on the surface quality (seven steps by 5° increments) when milling stainless steel. Results were supported also by the cutting force and residual stress measurements. It was concluded that the inclination angle change has a strong influence on the observed parameters and that very low inclination angles are not appropriate for achieving the desired results. It was mentioned that the tool geometry can also have influence, but no deeper analysis of this issue nor the optimal inclination angle proposal was drawn.

Based on the findings from many of these references, it is evident that a detailed understanding of the effects of parameter settings on the nature of surface roughness is very important for optimal setting of machining operations. If the point milling operation settings using the ball-end mill are unsuitable, then either the required surface roughness for the production of the part will not be achieved in many sections on the machined surface or, on the contrary, the resulting quality is too high in relation to the setting requirements. This can result in the production of a scrap part or, on the other hand, part production is too costly due to the increased production time and machine and tool costs. This waste machining time degrades the part material and wears out the tool. The area that has been least investigated to date is the setting of a suitable tool lead angle, which, if increased, would no longer cause such a pronounced influence on the required machined surface roughness perpendicular to the direction of the cutter movement which arises from the geometric indeterminacy of the engagement conditions near the tool centre. Different results can also be expected when using various types and diameters of the ball-end milling tools. Therefore, this paper aims to increase knowledge of the effects on the achieved surface roughness at a certain tool axis orientation angle and to deepen knowledge of the dependence of the achieved machined surface roughness on the input data that can be influenced when setting the toolpath, which in turn increases the reliability of achieving the required roughness in the transverse direction to the tool movement (i.e. transverse roughness).

2 Parameters and assumptions affecting transverse surface roughness

The analysis of the current state of the art shows that one of the main parameters directly influencing the machined surface's final transverse roughness is the actual effective tool cutting diameter at the contact point between the tool and the workpiece. The actual effective tool cutting diameter in turn directly affects the actual cutting speed at the contact

point. Specifically, with a ball-end mill, it is the section of the cutting edge defined by the original surface of the workpiece and the bottom of the toolpath, newly created during the point milling operation. However, the effect of the tool cutting edge geometry itself has not yet been analysed experimentally. It is therefore necessary to design a suitable experimental setup to analyse the transverse roughness achieved on the machined surface according to the actual tool lead angle relative to the machined surface, as well as the influence of the nominal diameter of the ball-end of the milling tool and of the cutting edge geometry itself.

A suitable experimental setup is shape machining where the tool contact point is variable depending on the workpiece shape. For simplicity, the machined specimens are considered as planar and the tool always has a fixed lead angle during milling, thus inducing specific contact point conditions as would occur at specific sections during machining of the shaped surface. The spindle speed is set so that the cutting speed on the tool diameter at the top of the machined groove is constant (Fig. 1), diameter at Sect. 3.
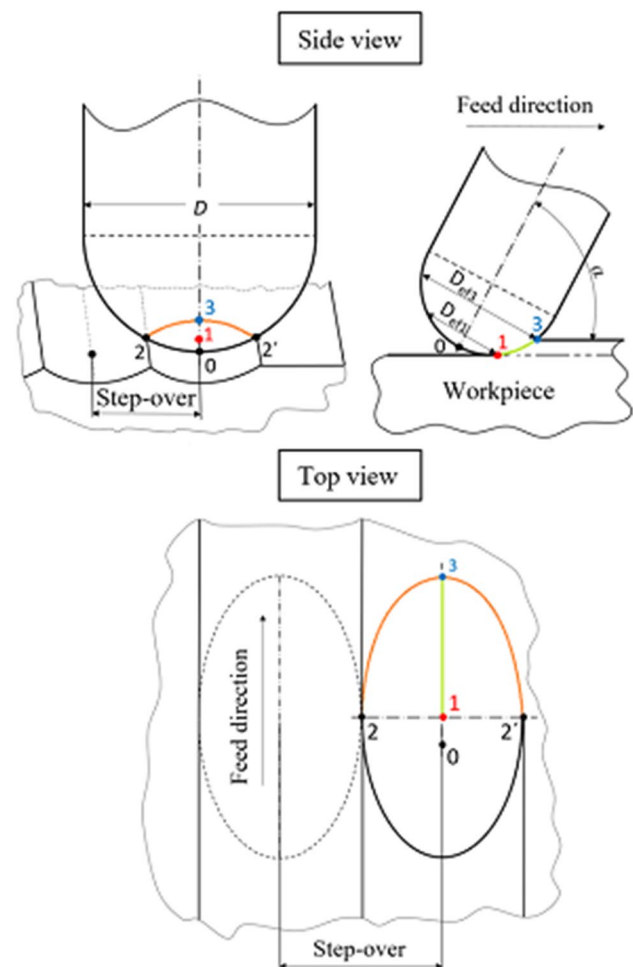

Fig. 1 Contact points of lead ball-end mill

Table 1 Cutting parameters for each tool

Tool diameter	Lead angle α (°)									
	0	1.5	2	2.5	3	3.5	4	7	10	30
	n (rev/min)									
D4	34,200	34,200	31,300	28,900	26,800	25,000	17,000	5800	4500	1900
D6	35,500	35,500	32,000	29,200	26,800	25,000	21,900	12,700	5300	4000
D8	36,300	36,300	32,500	29,400	26,800	24,700	22,800	12,200	5000	3800
D12	35,600	35,600	31,400	28,100	25,400	23,200	21,400	14,500	11,000	4400

For the case at hand, the effective diameter D_{ef} at a certain point of the cutting edge can be calculated according to Eq. (1) (equation can be found in [4] and in [18, Eq. 5]) when D is the nominal tool diameter (mm), α is the tool lead angle (°) and Sc is the selected scallop value (mm) (instead of Sc used in the case at hand any cutting depth may be used at which point it is desired to obtain the value of the effective diameter).

$$D_{ef} = D \times \sin\left[\alpha + \text{arc } \cos\left(\frac{D - 2 \times Sc}{D}\right)\right] \qquad (1)$$

The corresponding cutting speed v_c (m/min) at a given location is then calculated from Eq. (2), where n is the spindle speed (rpm).

$$v_c = \frac{\pi \times D_{ef} \times n}{1000} \qquad (2)$$

The four most common nominal diameters of the ball-end of the milling tool are chosen (see Table 1) and their effects on the achieved transverse roughness are analysed. To observe a lead angle value influence on the surface roughness, ten values of the lead angle setting are measured. For the smallest lead angle (or for zero), the value of the effective diameter reaches a minimum; and therefore, the cutting speed reaches a maximum. Here, the cutting speed is set to respect the spindle speed limit of the machine tool. Logically, a higher cutting speed can be set for higher tool diameters due to machining at higher effective diameters. The spindle speed for a particular tool at a particular lead angle setting is set to maintain a constant cutting speed at a corresponding effective diameter (calculated according to Eq. (2)). The depth of cut corresponds to the material removal during finishing, is set to one fixed value for all measurements and is set to the value $a_p = 0.1$ mm. Given the observation of the roughness parameter in a direction perpendicular to the tool movement (when the roughness in the groove is not observed), a constant feed per tooth is selected for machining (same for all the tool diameters: $f_t = 0.08$ mm) to prevent the possible influence of the feed rate change. All of the set parameters are summarised in Table 1.

A description of the contact points between the tool and the workpiece is presented as part of a more detailed analysis of the assumptions (Fig. 1). Parameter Sc is here equal to ap to simplify the scheme. The tool tip is represented by point 0 and the points on the left and right sides of the tool when moving through the groove are defined by points 2 and 2. The main points of observation in this experiment are marked 1 and 3. These are the points that include the minimum (point 1) and maximum (point 3) of the effective cutting diameter D_{ef}. The observed effective tool cutting diameter at these points is denoted as D_{ef1} and D_{ef3} and the corresponding cutting speeds v_{c1} and v_{c3}. In Fig. 2, a linear increase in the effective cutting diameter at both monitored points can be observed as a function of the lead angle for the selected nominal tool diameter D6. The linearly increasing trend in cutting speed v_{c1} must be reflected, while v_{c3} is constant (greater than the lead angle of 0°). The dependence of the cutting speeds on the lead angle at the two points for tool D6 can be seen in Fig. 3. These characteristics are related to the spherical shape of the ball-end mill envelope. The lead angles are set so that attention is paid to the section where other experiments have shown that there are significant changes in the resulting roughness. Lead angles greater than 4° are represented only by three additional values, as no significant difference in the resulting surface roughness is expected here.
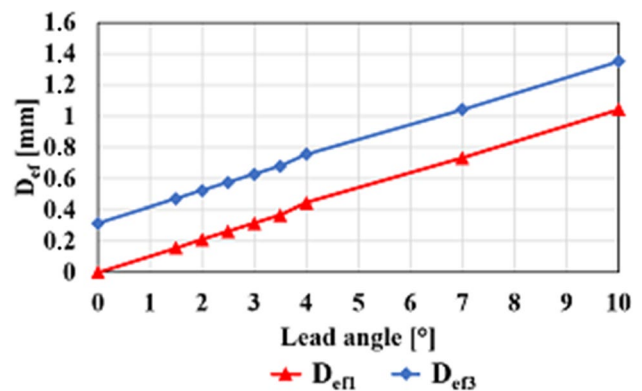

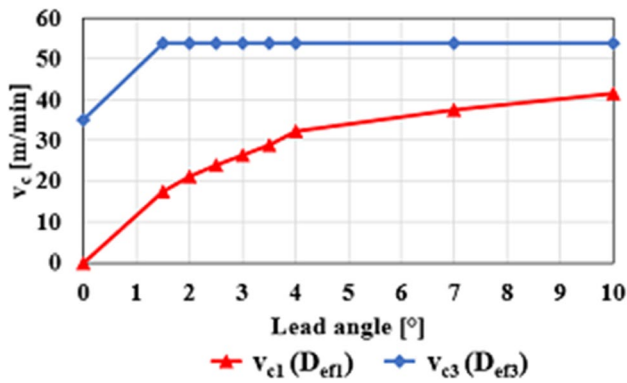**Fig. 2** Relation between lead angle and effective diameter D_{ef} (tool D6)

Fig. 3 Relation between lead angle and cutting velocity for certain D_{ef} (tool D6)

3 Experiment execution

The experiment design minimises the number of variable parameters that are not the main subject of investigation. The intention is to obtain results that can conclusively explain the influence of the monitored parameters on the resulting surface quality.

3.1 Workpiece material: tools and machine tool used

The chosen workpiece material is aluminium alloy with the designation EN-AW7075-T651. This alloy is often used in aerospace manufacturing and its advantages include high tensile strength, good machinability and low weight. It is assumed that for this material, the effect of cutting conditions on the intensity of cutting edge wear will be negligible, thus excluding the effect of wear in the experiment measurements. The material does not tend to adhere to the cutting edge, which could potentially affect the machined surface. The blank is a drawn flat bar pre-machined to $190 \times 110 \times 25$ mm. The test blank is provided with a pair of through-holes for M8 countersunk head screws. These screws are used to clamp the blank to the machine table via the stones in its T-slots. Emulsion liquid (Blasocut Combi) at a concentration of 5% is used for cooling during machining, and the supply to the cut is provided by two external nozzles. For the experiment, double-bladed uncoated cylindrical shank ball-end milling tools from ISCAR with a grade of IC08, nominal diameters of 4, 6, 8 and 12 mm and overall lengths of 50, 51, 63 and 71 mm were chosen. The specific manufacturer code designations are EB-A2 04-06C06E50, EB-A2 06-07C06E51, EB-A2 08-09C08E63 and EB-A2 12-14C12E71. Thermal clamps were selected for tool clamping. The experiment was carried out on a five-axis MCVL1000 milling centre (manufactured by KOVOSVIT MAS Machine Tools) equipped

with a NIKKEN tilt-turn table. The working range of the machine tool is $X = 1016$ mm, $Y = 610$ mm and $Z = 660$ mm. The range of working feeds of all machine axes is identical: 2 to 12,000 mm/min. The electric spindle of the machine with the HSK E40 clamping interface has a maximum speed of 42,000 rpm.

3.2 Toolpaths and chosen strategy

One square sample is machined for each tool and lead angle combination. The set of samples is evenly distributed on the face of the blank. The dimension of one machined sample is 7×7 mm, with the exact scallop value based on Eq. (3) (equation can be found in [3, Eq. 1], [4] and in [25, Eq. 1]), where Rsm (spacing of the grooves according to ISO 4287) is rounded down to make the sample width an integral multiple thereof (in the case at hand the spacing of the grooves is represented by the step-over parameter set by the NC programmer). The tool movement (Fig. 4) is based on a zig strategy with a left-to-right rowing direction to ensure climb cut (down milling). The desired workpiece tilt orientation is set by indexing the table by tilting it in the B axis. The toolpath for milling samples is implemented through interpolation of the X and Z axes and the step-over direction takes place in the Y axis.

$$Sc = \frac{D}{2} - \frac{\sqrt{D^2 - Rsm^2}}{2} \tag{3}$$

3.3 Selection of the lead angle

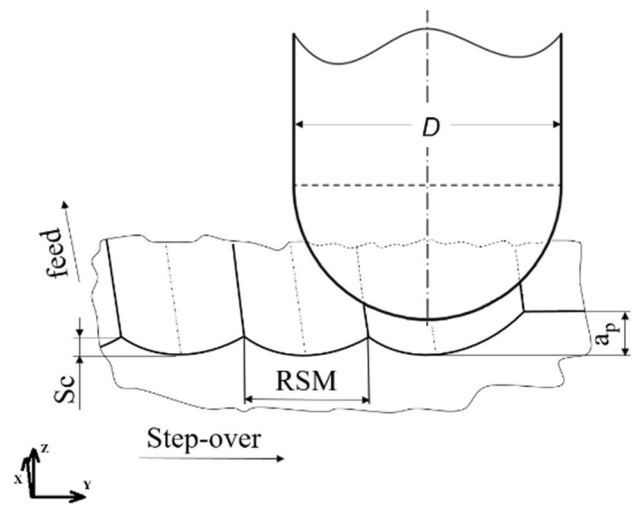The logic used to set the lead angle change was that the discrepancy between the desired and actual measured surface

Fig. 4 Step-over diagram

roughness would be highest for small angles; therefore, the lead angle change is set with a small spacing for small angles. For larger lead angles, the assumption is that the surface roughness results would be relatively constant. Thus, there is no bigger setting step change in this range of angles. To ensure constant cutting edge engagement conditions, one tool orientation variation was chosen, namely pull milling.

3.4 Implementation of the experiment

Before machining, the cutting edge envelopes of the ball-end milling tools were measured. They deviated from the ideal nominal ball by -0.006 to $+0.006$ mm with respect to the nominal diameter. The radial runout of the tools clamped in the chuck and into the machine spindle was also measured to eliminate the effect of runout on the measurements. The tool radial runout during all tests ranged from 0.005 to 0.008 mm. The machine tool setup during sample milling with the D12 ball-end mill is shown in Fig. 5.

3.5 Tool analysis

The actual tool cutting edge geometry was determined with an Alicona InfiniteFocus G5 scanning digital microscope. The cutting edges of each milling tool were analysed by converting the STL file into CAD software. Differences in the geometry of the cutting edges, which were sharpened on

the individual tools, may affect the differing texture of the resulting machined surface of the samples.

The surface roughness of the samples was measured using a Mahr LD130 roughness instrument with an LP C 25–15-2_90 measuring transducer. The characteristics were evaluated according to ISO 4287, using a Gaussian filter ISO 16610–21 with a cutoff wavelength LC of 0.8 mm. Roughness measurements were performed perpendicular to the direction of tool movement in the trace (as shown on Fig. 6). The texture of the machined surface on the samples was also optically observed on a KEYENCE VHX-7000 microscope (Fig. 7) with a VH-ZST Dual objective zoom lens. For the sample surface scanning, a Keyence VK-X1100 confocal microscope was used.

4 Results and discussion

The following tables show the measurements of the roughness parameters Rz (Table 2) and Ra (Table 3) for the tool lead angles that had been set. These are the averages of five repeated measurements on each sample. The reason why the Rz parameter was evaluated is that it represents the arithmetic mean value of the depth of roughness on the measured profile (important for checking the part for compliance with the drawing requirements). $Rmax$ parameter was also observed and results showed consistent values that differed by less than 10% from the Rz, which indicates

Fig. 5 Milling experiment (tool D12)

Fig. 6 Surface roughness measurement on the sample (using the Mahr instrument)

Fig. 7 Optical surface measurement (using the KEYENCE microscope)

the stability of the depth of roughness on the measured profile (the results are not tabulated, as the parameter is not the main focus of the observation). In Table 2, the scallop values *Sc* are also indicated.

Figure 8 shows the dependence of parameter $\mathcal{E}_{sc}$ on lead angle change. $\mathcal{E}_{sc}$ is the ratio of the *Rz* measurements to the set *Sc*, and hence the relationship between the actual measured data and the parameter set for the measurement, as stated in Eq. (4). The desired ratio is therefore equal to 1, and it therefore helps to unify the results of individual tool diameters into a common (dimensionless) system of values. The figure shows the lead angle range up to 8°; for larger lead angles, the constant value of (epsilon) was achieved. The larger the tool diameter, the larger the difference between the measured *Rz* and scallop for a given lead angle. However, this type of dependence was not found for the D6 tool, which exhibits a relatively consistent $\mathcal{E}_{sc}$ ratio over the entire range of selected lead angles. It is also evident that for the diameters of tools D8 and D12, the measured *Rz* corresponds to the theoretical *Sc* value only with larger lead angles than for tools D4 and D6. For all tools, it was true that from a certain

Table 2 *Rz* parameter measurements

Tool diameter	Lead angle α (°)										Sc (µm)
	0	1.5	2	2.5	3	3.5	4	7	10	30	
	Rz (µm)										
D4	5.28±0.05	6.03±0.05	5.91±0.08	5.92±0.13	5.76±0.1	5.47±0.05	4.93±0.05	4.19±0.06	4.18±0.07	4.53±0.03	4.2
D6	5.22±0.17	5.09±0.2	4.94±0.24	4.66±0.24	4.92±0.23	5.02±0.2	5.1±0.25	4.51±0.1	4.53±0.17	4.48±0.12	4.1
D8	7.95±0.28	7.65±0.09	7.69±0.3	7.20±0.31	6.46±0.33	5.38±0.25	4.74±0.3	4.47±0.25	4.48±0.12	4.42±0.1	4.4
D12	10.86±0.5	11.63±0.41	10.99±0.48	11.09±0.35	10.22±0.31	9.00±0.32	6.89±0.42	4.40±0.35	4.57±0.4	4.68±0.43	4.5

Table 3 *Ra* parameter measurements

Tool diameter	Lead angle α (°)									
	0	1.5	2	2.5	3	3.5	4	7	10	30
	Ra (µm)									
D4	1.29±0.02	1.30±0.07	1.31±0.1	1.34±0.15	1.34±0.08	1.26±0.07	1.12±0.07	1.01±0.03	1.01±0.02	1.08±0.01
D6	1.39±0.07	1.26±0.05	1.16±0.04	1.10±0.08	1.07±0.04	1.14±0.05	1.11±0.09	1.03±0.03	1.07±0.07	1.04±0.02
D8	2.05±0.17	1.93±0.05	2.02±0.15	1.97±0.13	1.59±0.14	1.21±0.1	1.09±0.1	1.03±0.15	1.05±0.07	1.05±0.05
D12	2.87±0.2	3.09±0.21	2.75±0.12	2.70±0.07	2.45±0.13	2.14±0.15	1.59±0.17	0.95±0.08	1.04±0.1	1.07±0.09
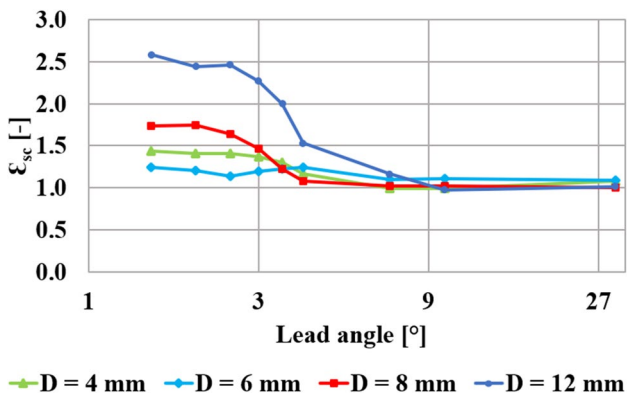
Fig. 8 Characteristic of the parameter ε_{sc} in relation to the lead angle

threshold lead angle, the ε_{sc} ratio was close to the desired value of 1 for all higher values. To determine the nature of this phenomenon, the geometry of the spherical part of the tools of all diameters is analysed in the next step.

$$\varepsilon_{sc} = \frac{Rz}{Sc} \tag{4}$$

The tool-cutting edge geometry was evaluated in the tool tip area corresponding to the lead angle where the change in the achieved transverse roughness had been found. Figure 9 highlights the two main tool surface areas: rake face (2) and primary relief (3). A detailed analysis of the cutting edge geometry of the tools of all diameters showed design differences in the transitional part of the blade (the outline of the blade around the tool axis). This detail can be described by the circle (1), hereinafter referred to as the circular transition boundary.

Figure 10 highlights the material removal zone for tool lead D6 at an angle of 3°. The area boundary diameters are D_{ef1} (inner) and D_{ef3} (outer), as shown in Fig. 1. In this case, the circle *C1* (1) created by tool sharpening does not interfere with the contact area (2).
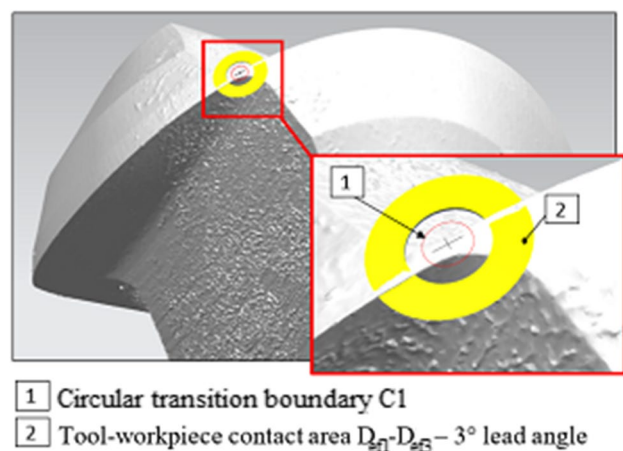

1 Circular transition boundary
2 Rake face
3 Primary relief

Fig. 9 Description of ball mill geometry elements

1 Circular transition boundary C1
2 Tool-workpiece contact area D_{ef1}-D_{ef3} – 3° lead angle

Fig. 10 Observations of tool geometry (D6) and tool-workpiece contact for a lead angle of 3°
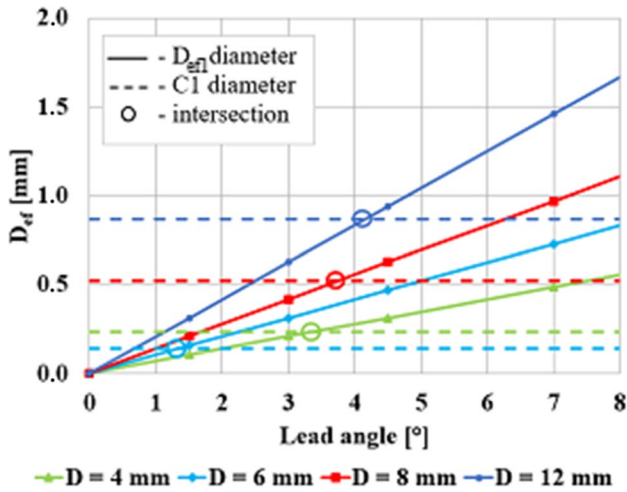
Fig. 11 Comparison of diameter of grinded edge and effective diameters

Table 4 Measured diameters *C1* and the limit lead angles for each tool diameter

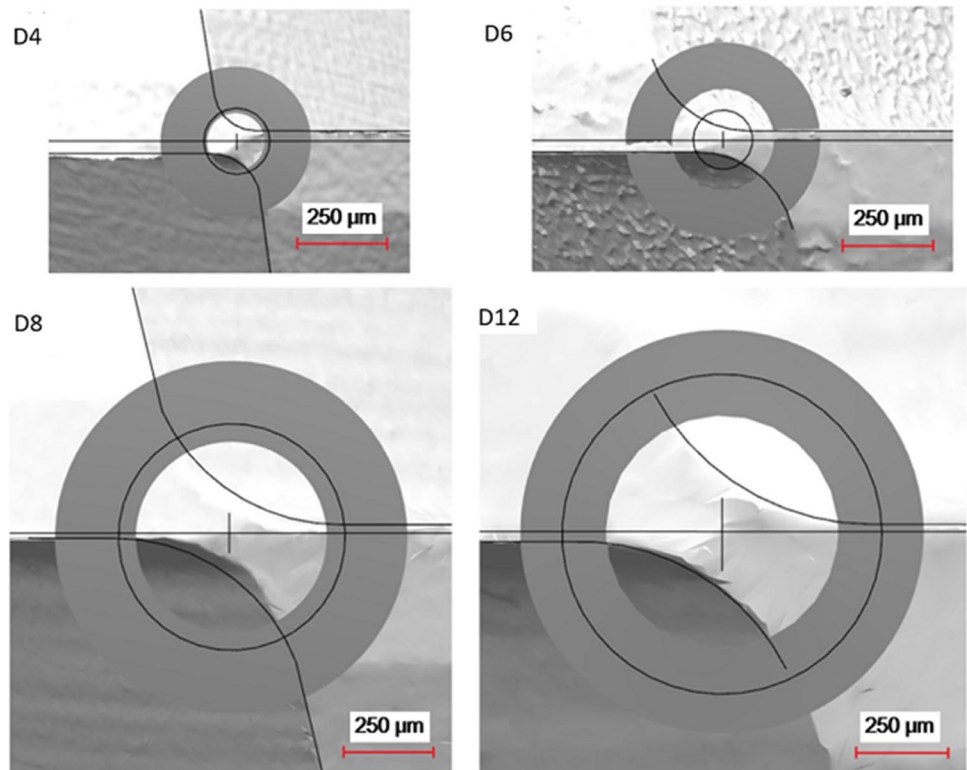| Tool diameter	C1 (mm)	Limit lead angle (°)
D4	0.24	3.3
D6	0.14	1.3
D8	0.52	3.7
D12	0.87	4.1

Figure 11 shows a comparison of the effective cutting diameters D_{ef1} for lead angles ranging from 0° to 8°. The measured significant diameters of the grinded geometry transition *C1* for each tool are indicated (horizontal dashed line). The D6 tool has a circle intersection with the engagement zone close to the 1.5° lead angle. The other tools have a circle intersection with the engagement zone at a greater lead angle value (between 3° and 4.5°).

Table 4 summarises the measured diameters *C1* for each tool diameter and the exact values of limit lead angles obtained by comparing the *C1* values and the dependence of diameter D_{ef1} on the lead angle.

Figure 12 shows the contact zone for a lead angle of 3° and the circle *C1*, corresponding to the circular transition boundary. For tools D4, D8 and D12, the contact zone and circle *C1* intersect, and for tool D6, this circle does not interfere with the contact zone. As shown in Fig. 13, this is the cause of the poor surface roughness and the significant increase in $\mathcal{E}_{sc}$ above 1, as shown in the graph in Fig. 8. The interference of the cutting edge section with the circular transition boundary causes irregular tool marks on the machined surface (for all tools except D6 in this case), and this leads to an increase in *Rz* compared to the predicted *Sc* value. The larger the area of this part of the tool cutting edge that performs chip removal, the higher the resulting $\mathcal{E}_{sc}$ value; see Fig. 8.

Figure 14 shows the contact zone for a lead angle of 4° and the circle *C1*, corresponding to the circular transition

Fig. 12 Axial view of the tool geometry—section of cutting edge for the lead angle range of 3° (for tools D4, D6, D8, D12)

Fig. 13 Finished surfaces by 3° lead angle for the four cutting tool diameters (D4, D6, D8, D12)
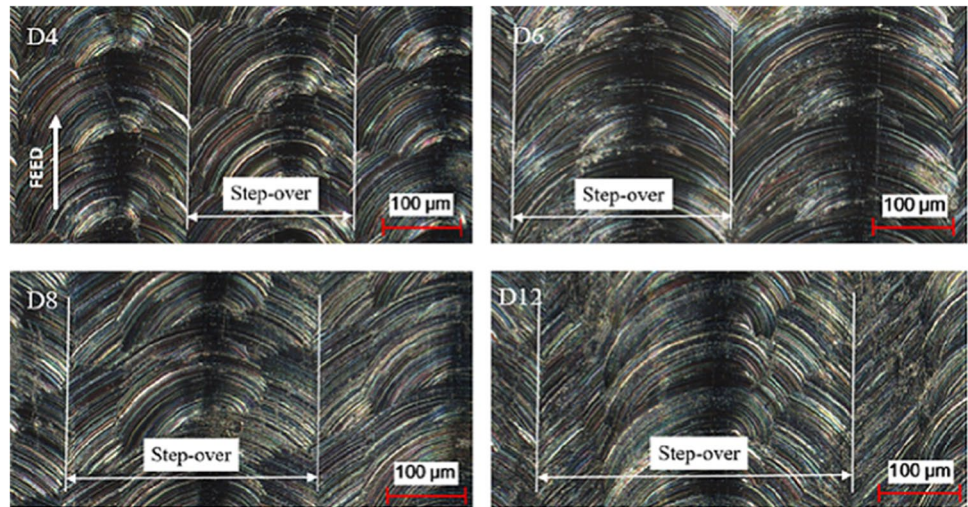
boundary. In the case of tool D12, the contact zone and circle *C1* intersect; for tools D4, D6 and D8, this circle does not interfere with the contact zone. Figure 15 shows that for the surfaces finished with tools D4, D6 and D8, the tool trace has a regular form, while the undesired tool impression is still present in the tool D12 sample. This corresponds to the $\mathcal{E}_{sc}$ value, which is still quite high for tool D12 (over 1.5). On the other hand, for the other tool samples, the $\mathcal{E}_{sc}$ value achieves a constant level even for larger lead angles, i.e. close to the desired value of 1, as shown in the graph in Fig. 8.

The observed relationship between the shape and regularity of the marks left by the ball-end mill during leading on the machined surface and the contact point between the tool and the workpiece is consistent with the observed dependencies of the surface roughness measurements and $\mathcal{E}_{sc}$ ratio for a particular lead angle setting. The results point to the conclusion that for a given tool geometry, the diameter *C1* may be determined by analysing the tool cutting edge shape. Using this diameter, it is possible to derive the minimum tool lead angle from which the transverse roughness of the

Fig. 14 Axial view of the tool geometry—for the section of cutting edge in the lead angle range of 4° (for tools D4, D6, D8, D12)
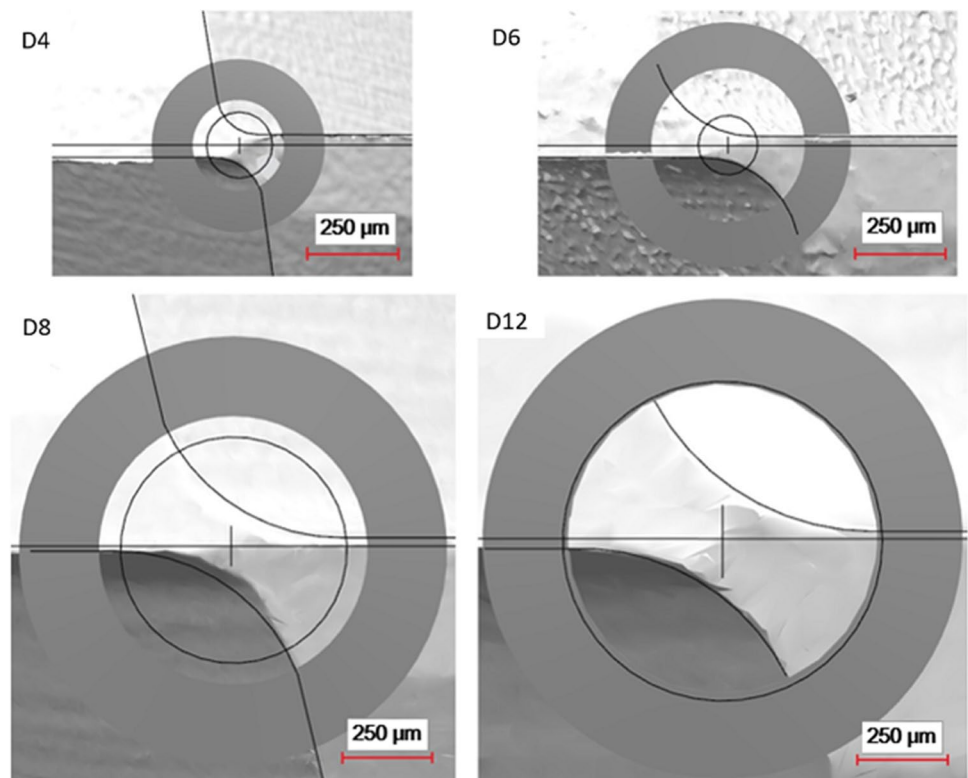
Fig. 15 Finished surfaces by 4° lead angle for the four cutting tool diameters (D4, D6, D8, D12)
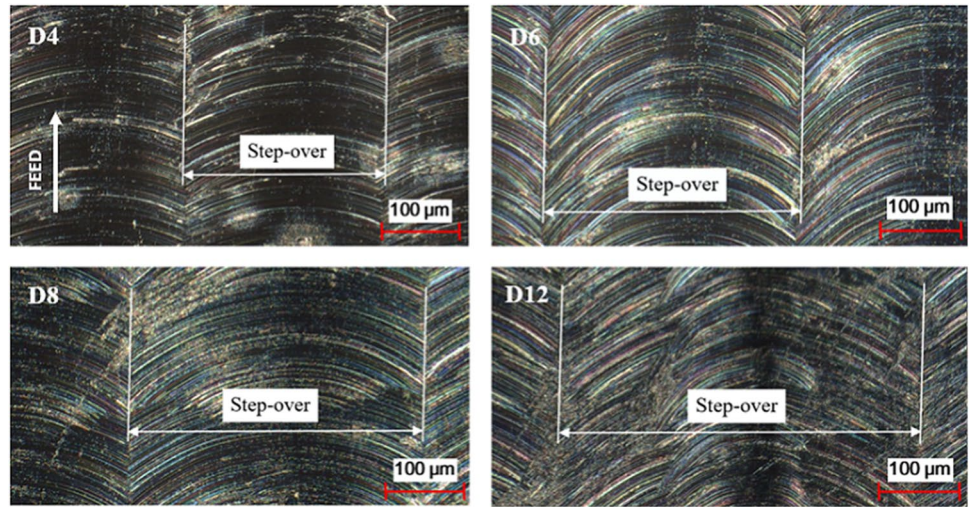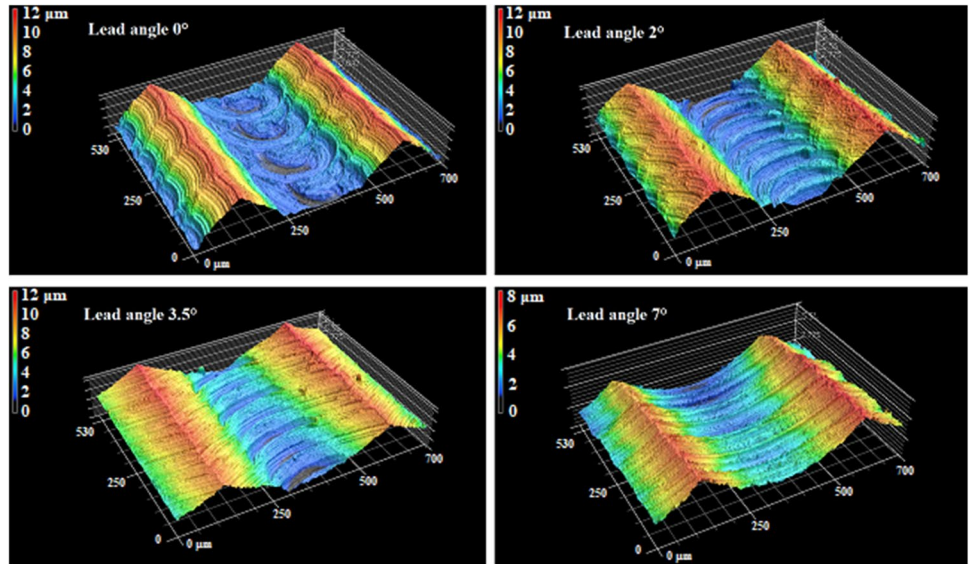

Fig. 16 Scanned surface pictures on confocal microscope (D12 tool samples—lead angle 0°, 2°, 3.5°, 7°)

machined surface will correspond to the value which is a theoretical assumption based on the tool path setting. In contrast, it is evident that this value is independent of the nominal tool diameter.

As seen in Fig. 16, the marks on the bottom of the groove disappear with increasing values of the lead angle (illustrated case of the D12 tool). These marks have a direct correlation with the tool geometry in the specific cutting area of the cutting edge and cause the groove to deepen. When the marks are not notable also the groove depth is shallow (corresponds to the assumption).

The results of the surface roughness measurements also indicate the possibility of determining the ratio of two surface roughness parameters—Rz and Ra. This ratio (Fig. 17) is constant even for small lead angles, although here the dependence is not completely linear (the X-axis is truncated, while the other measured values are constant).

Thus, Ra can be derived from this ratio for the given conditions if we know Rz or scallop (parameter Sc). The relationship between Rz and Ra is tentatively defined by the
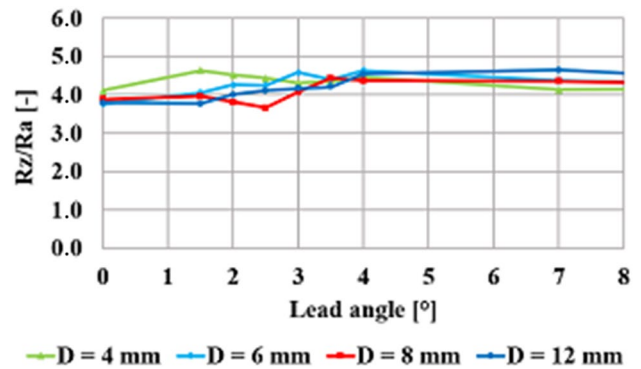

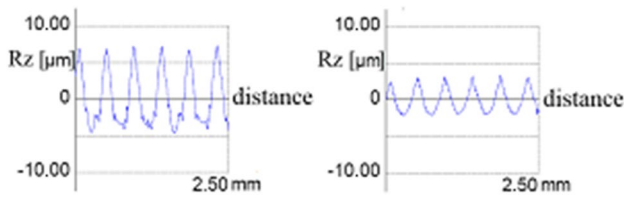**Fig. 17** Dependence of the Rz/Ra ratio on the lead angle

Fig. 18 Measured profile of surface topography for D12 tool: lead angle of 1.5° (left), lead angle of 4.5° (right)

standard [DIN 4768]. The results thus signify a significant refinement of parameter dependence. The larger the Rz, the larger the Ra (valid for all cutter diameters). As the lead angle increases above the point where the $\mathcal{E}_{sc}$ ratio stabilises close to 1, the Rz/Ra ratio varies between 4.1 and 4.6. When the lead angle is below this limit, the Rz/Ra ratio range increases to between 3.7 and 4.6. In general then, if Rz is known, the Ra for the least favourable case can be determined for a given setup by the formula $Ra = Rz/3.8$.

The parameter Ra is the average arithmetic roughness value. It can be obtained as the arithmetic mean of all parts of the roughness profile values according to ISO 4287. When comparing the Ra parameter for different roughness profiles, the amplitude of the profile and the nature of the profile in the regions between the amplitudes are important. The parameter Rz represents the depth of roughness, namely the arithmetic mean of the different depths of roughness Rzi occurring in the measured section of the profile. The parameter Rz, unlike Ra, only considers the values of the profile amplitudes in the given profile sections, not the nature of the profile between amplitudes.

Figure 18 illustrates why the Rz/Ra ratio is constant even when the measured Rz differs significantly from the theoretical scallop value. The two profiles of the measured roughness for lead angles of 1.5° and 4.5° show that although the peak amplitudes are different, their frequencies (parameter Rsm) and especially the waveforms are identical. Under these assumptions, it follows that whatever the amplitude of the peaks, the average Ra value will always be the same multiple of the value of that amplitude (hence Rz).

5 Conclusion

The machined surface roughness on the shaped part perpendicular to the tool movement can be influenced by various parameters. In this experiment, attention was paid to lead angle variation for four selected ball-end mill diameters. The other machining parameters were held constant to eliminate other effects on machined surface roughness.

1. The result shows a discrepancy between the theoretical scallop roughness value and the actual measured parameter Rz ($\mathcal{E}_{sc}$ ratio), where for small lead angles, the measured Rz value is higher than the theoretical value resulting from the setting of the machining strategy and the applied conditions.
2. The result further leads to the finding that the specific tool geometry influences the possibility of achieving the required surface roughness, rather than a low cutting speed on a small effective diameter (the actual diameter of the tool-workpiece contact). It is not the nominal diameter that plays a role, but the particular cutting edge geometry on the affected effective diameters.
3. If the resulting chip is also generated by the curling part below the circular transition boundary, the surface has an irregular character. As a consequence, the real surface roughness Rz does not correspond to the theoretical (expected) value. An important and new finding is therefore that for a given tool, it is possible to find, from a simple macroscopic analysis of its geometry, an effective diameter which determines the limiting minimum tool lead angle from which the transverse roughness of the machined surface will correspond to the value which is theoretically required during pre-production setting of toolpath and cutting conditions. This can significantly help technologists efficiently set milling operations and avoid repeated re-setting for better machining results.
4. Another advantage is that the results also allow a general and relatively accurate determination of the Rz/Ra ratio when milling EN AW 7075 material with a ball-end milling tool. The obtained ratio applies to all of the tools used.

Data availability Not applicable.

Code availability Not applicable.

Declarations

Ethics approval Not applicable.

Consent to participate Not applicable.

Consent for publication Not applicable.

Competing interests The authors declare no competing interests.

References

1. Chen J-S, Huang Y-K, Chen M-S (2005) A study of the surface scallop generating mechanism in the ball-end milling process. Int J Mach Tools and Manuf 45(9):1077–1084
2. Chen X, Zhao J, Dong Y, Han S, Li A, Wang D (2012) Effects of inclination angles on geometrical features of machined surface in five-axis milling. Int J Adv Manuf Technol 65:1721–1733
3. Stahovec J, Kandráč L (2013) Optimization of cutting conditions for the reduction cusp height in the milling process. Transfer Inovácií 25:244–248
4. Mikó B, Beňo J (2014) Effect of the working diameter to the surface quality in free-form surface milling. Key Eng Mater 581:372–377
5. Vijayaraghavan A, Hoover AM, Hartnett J, Dornfeld DA (2009) Improving endmilling surface finish by workpiece rotation and adaptive toolpath spacing. Int J Mach Tools Manuf 49:89–98
6. Batista M, Rodrigues A, Coelho R (2015) Modelling and characterisation of roughness of moulds produced by high-speed machining with ball-nose end mill. Proc Inst Mech Eng Part B J Eng Manuf 231:933–944
7. Batista M, Brandão L, Coelho R (2005) The influence of some cutting parameters in finishing milling of hardened steel using ball nose tool, in *Proc.* COBEM, Ouro Preto
8. Mali R, Aiswaresh R, Gupta T (2020) The influence of tool-path strategies and cutting parameters on cutting forces, tool wear and surface quality in finish milling of Aluminium 7075 curved surface. Int J Adv Manuf Technol 108:589–601
9. Mikó B, Zentay P (2019) A geometric approach of working tool diameter in 3-axis ball-end milling. Int J Adv Manuf Technol 104:1497–1507
10. Souza AD, Berkenbrock E, Diniz A, Rodrigues A (2015) Influences of the tool path strategy on the machining force when milling free form geometries with a ball-end cutting tool. J Braz Soc Mech Sci Eng 37:675–687
11. Scandiffio I, Diniz A, Souza AD (2017) The influence of tool-surface contact on tool life and surface roughness when milling free-form geometries in hardened steel. Int J Adv Manuf Technol 92:615–626
12. Beňo J, Maňková I, Ilžo P, Vrabel M (2016) An approach to the evaluation of multivariate data during ball end milling free-form surface fragments. Measurement 84:7–20
13. Aspinwall D, Dewes R, Ng E-G, Sage C, Soo S (2007) The influence of cutter orientation and workpiece angle on machinability when high-speed milling Inconel 718 under finishing conditions. Int J Mach Tools Manuf 47:1839–1846
14. Wojciechowski S, Twardowski P, Wieczorowski M (2014) Surface texture analysis after ball end milling with various surface inclination of hardened steel. Metrol Meas Syst 21(1):145–156
15. Wojciechowski S, Marida R, Barrans S, Nieslony P, Krolczyk G (2017) Optimisation of machining parameters during ball end milling of hardened steel with various surface inclinations. Measurement 111:19–28
16. Vavruska P, Zeman P, Stejskal M (2018) Reducing machining time by pre-process control of spindle speed and feed-rate in milling strategies. Procedia CIRP 77:578–581
17. Käsemodel R, Souza AD, Voigt R, Basso I, Rodrigues A (2020) CAD/CAM interfaced algorithm reduces cutting force, roughness, and machining time in free-form milling. Int J Adv Manuf Technol 107:1883–1900
18. Erdim H, Lazoglu I, Ozturk B (2006) Feedrate scheduling strategies for free-form surfaces. Int J Mach Tools Manuf 46:747–757
19. Rybicki M (2014) Problems during milling and roughness registration. J Phys Conf Ser 483:012007
20. Matras A, Zebala W (2020) Optimization of cutting data and tool inclination angles during hard milling with CBN tools based on force predictions and surface roughness measurements. Materials 13(5):1109
21. Lazoglu I, Manav C, Murtezaoglu Y (2009) Tool path optimization for free form surface machining. CIRP Ann 58(1):101–104
22. Costes J, Moreau V (2011) Surface roughness prediction in milling based on tool displacements. J Manuf Process 13:133–140
23. No T, Gomez N, Smith S, Schmitz T (2020) Cutting force and stability for inserted cutters using structured light metrology. Procedia CIRP 93:1538–1545
24. Tunc L-T (2019) Smart tool path generation for 5-axis ball-end milling of sculptured surfaces using process models. Robot Comput Integr Manuf 56:212–221
25. Mikó B, Beňo J, Maňková I (2012) Experimental verification of cusp heights when 3D milling rounded surfaces. Acta Polytech Hung 9:101–116
26. Shchurov I, Al-Taie L (2017) Constant scallop-height tool path generation for ball-end mill cutters and three-axis CNC milling machines. Procedia Engineering 206:1137–1141
27. Liu W, Zhu S-M, Huang T, Zhou C (2020) An efficient iso-scallop tool path generation method for three-axis scattered point cloud machining. Int J Adv Manuf Technol 107:3471–3483
28. Liu W, Z L-S, An L-L (2012) Constant scallop-height tool path. Int J Adv Manuf Technol 63(1–4):137–146
29. Yang L, Wu S, Liu X, Liu Z, Zhu M, Li Z (2018) The effect of characteristics of free-form surface on the machined surface topography in milling of panel mold. Int Adv Manuf Technol 98:151–163
30. Quinsat Y, Sabourin L, Lartigue C (2015) Surface topography in ball end milling process: description of a 3D surface roughness parameter. J Mater Process Technol 195(1–3):135–143
31. Sekine T (2021) Comparative study on path interval and two tool condition parameters in ball and filleted end milling. Adv Sci Technol Res J 15:311–320
32. Sekine T (2021) Theoretical approaches for determining machining conditions affecting a machined surface topography in filleted end milling. Adv Model Optim Manuf Process 12:123–132
33. Lofti S, Rami B, Maher B, Gilles D, Wassila B (2018) An approach to modeling the chip thickness and cutter workpiece engagement region in 3 and 5 axis ball end milling. J Manuf Process 34:7–17
34. Zhang X, Zhang J, Zheng X, Pang B, Zhao W (2018) Tool orientation optimization of 5-axis ball-end milling based on an accurate cutter/workpiece engagement model. CIRP J Manuf Sci Technol 19:106–116
35. Jang G, Yu N, Hwang H, Jang G, Bang T (2021) Calculating method of tool tilt angle by solving of quadratic equations in 5-axis machining with flatend cutter. Lond J Eng Res 21:788–801
36. Matras A (2015) The influence of tool inclination angle on the free form surface roughness after hard milling, in *Proc*. SPIE, San Diego
37. Stejskal M, Vavruska P, Zeman P, Lomicka J (2021) Optimization of tool axis orientations in multi-axis toolpaths to increase surface quality and productivity. Procedia CIRP 101:69–72
38. Sadilek M, Cep R (2009) Progressive strategy of milling by means of tool axis inclination angle. World Acad Sci Eng Technol 53:135–139